A Modelling-Mapping Approach for Fine-Scale Natural Ventilation Evaluation in High Density Cities

Chao Yuan[1, 2], Leslie Norford[3], Rex Britter [4], Steve Yim[5] , Edward Ng[6],

1 Massachusetts Institute of Technology, 77 Mass. Ave, Cambridge, MA, US. yuanc@mit.edu
2 Singapore University of Technology and Design, 8 Somapah Rd, Singapore. yuanc@mit.edu
3 Massachusetts Institute of Technology, 77 Mass. Ave, Cambridge, MA, US. lnorford@mit.edu
4 Massachusetts Institute of Technology, 77 Mass. Ave, Cambridge, MA, US. rexb@mit.edu
5 The Chinese University of Hong Kong, Shatin, Hong Kong. steveyim@cuhk.edu.hk
6 The Chinese University of Hong Kong, Shatin, Hong Kong. edwardng@cuhk.edu.hk
dated: 27 June 2015

1. Introduction

Due to rapid urbanization and depletion of natural resources, high-density urban living to make better use of natural resources is an inevitable growing trend. However, closely packed high-rise buildings often result in stagnant airflow in high-density urban areas, which has been associated with increased exposure to ambient air pollution and outdoor thermal discomfort. From the perspective of outdoor thermal comfort, Cheng et al. (2011) indicated that a decrease in wind speed from 1.0 to 0.3 meter/second is equivalent to a 1.9°C increase in ambient temperature and a wind speed of about 1.6 m/s is required to achieve neutral thermal sensation in subtropical areas during summer. Decreasing wind speed has also been shown to lower the convective effect of ambient air pollutant dispersion (Tominaga and Stathopoulos, 2011). Therefore, improvement of the wind environment in urban areas using wind flow and dispersion information is among the fundamental tasks of high-density urban planning.

In this study, we aim to develop a fine-scale morphological modelling-mapping approach to provide pedestrian-level wind information between buildings, which could enable more efficient decision-making in urban planning and design. This approach not only could avoid the high simulation costs of Computational Fluid Dynamics (CFD) (Tominaga et al., 2008), it could also increase the resolution of the wind environment map to several meters, compared with the hundred meters resolution in the conventional morphological models (Grimmond and Oke, 1999; Ng, et al., 2011). As a result, our new approach could bridge the gap between the current modelling methods and requirements of practical planning and design.

2. Development of a morphological model for fine-scale wind estimation

In order to address the limitations of both CFD simulation and conventional morphological models, we developed a refined morphological model that provides high spatial resolution wind information at the pedestrian level between buildings without increasing the computational cost. The modelling was based on developing approximations to avoid directly calculating the flow between roughness elements. As Belcher et al. (2003) did, we assumed the flows in a fully developed atmospheric boundary layer, with wind components, $U_{(z)}$ (u, 0,0), in urban areas with annual wind frequency (pi) for 16 wind directions (i=1,…,16).

First, we related the pedestrian-level wind speed to building frontal area density (λ_f) over a certain height range (Δz) as averaged over a high density area, based on the understanding of momentum transfer and drag force balance in the canopy layer (Bentham and Britter, 2003; Coceal and Belcher, 2004). MacDonald et al. (1998) indicated that the λ_f^* [frontal area density above the displacement height (z_d)] can better estimate the wind profile than conventional λ_f; on the other hand, the near-ground wind speed depends on the λ_f' (frontal area density below z_d), instead of λ_f^*. Ng et al. (2011) defined the podium layer (0m -15m) in Hong Kong due to the podium morphological characteristic, and considered that the air is impeded at the podium layer as much as if it is under z_d. The wind velocity ratio (VR) is well related to λ_f' ($\lambda_{f(0-15m)}$: frontal area density in the podium layer), rather than λ_f^* ($\lambda_{f(15-60m)}$: frontal area density in the building layer). Since we chose Hong Kong as the target city, λ_f' calculated from 0m to 15m is applied in this study.

Second, we adjusted the morphological index λ_f' using the distance from roughness elements to target points to estimate the fine-scale wind speed between roughness elements. Here, we illustrate how air flows through urban areas by describing the momentum transfer and drag force balance in a moving air parcel. The air parcel is impeded by the drag force of roughness elements, and is accelerated by the downward transfer of horizontal momentum. It means that the parcel will stop without vertical transfer of horizontal momentum (Belcher et al., 2003). The speed of the air parcel can be recovered after traveling further away from the roughness element. It indicates that, when the wind speed at test points is affected by the surrounding area, the effects of individual roughness elements are different, given that the distances from the target point to individual roughness elements are different. Consequently, we create a distance index (L) and calculated the point-specific frontal area density ($\lambda_{f\text{-point}}$) by adjusting λ_f' using the distance index (L). This adjustment of calculation indicates that $\lambda_{f\text{-point}}$ is not only spatially and annually averaged but also point-specific. As shown in Figure 1, frontal area pixels in Δz (0m -15m) ($A_{\Delta z,i}$), weighted by the distance coefficient (l) and annual wind frequency (pi) in the ith wind direction, were added up and normalized by the scanned area to calculate the point-specific frontal area density ($\lambda_{f\text{-point}}$) as:

$$\lambda_{f\_point} = \frac{\iint_D l_{x,y}^{c}(A_{\Delta z,x,y}/A_t)dxdy}{A_t},\ D = \{x^2 + y^2 \le r^2\} \quad (1)$$

$$A_{\Delta z,x,y} = \sum_{1}^{i=16} A_{\Delta z,i} p_i \quad (2)$$

$$l_{x,y} = \frac{r - L}{r} \quad (3)$$

$$A_t = \pi \cdot r^2 \quad (4)$$

where $A_{\Delta z,x,y}$ is the wind frequency-weighted frontal area at the pixel (x, y), in which x and y are the coordinates, Δz is from 0-15 m (Ng et al., 2011), and $l_{x,y}$ is the distance coefficient. The A_t is the scanned area and r is the scan radius (200 m) (Ng et al., 2011), as shown in Figure 1. Belcher et al. (2003) indicated that the increase of the mean wind speed is not linear when the air parcel moves further away from the roughness elements. Therefore, an exponent c, 2.0, is used to adjust $l_{x,y}$. As indicated in Table 1, the modelling results with the exponent c=2.0 fit the experimental data better than the one with the exponent c=1.0.

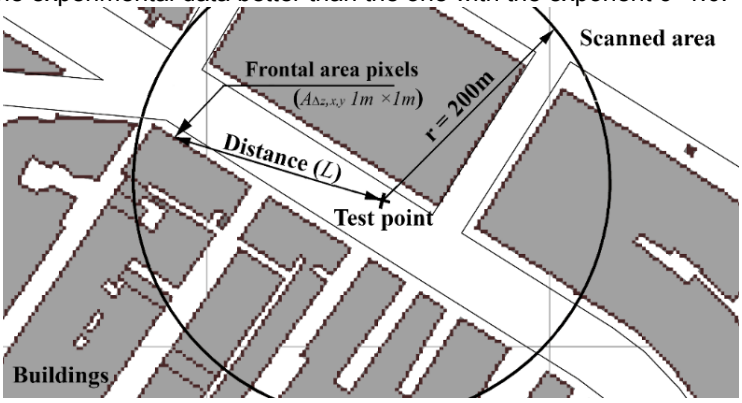

Figure 1 Schematic illustration of $\lambda_{f\text{-}point}$ calculation. Test point, scanned area (A_t), radius (r), distance (L), and frontal area units (red pixels) at the boundaries of buildings are presented.

3. Model testing

We correlated the wind tunnel data with the point-specific index ($\lambda_{f\text{-}point}$) to test the model performance. First, we obtained the overall wind VR measured in a wind tunnel experiment conducted by the Hong Kong Planning Department (Hong Kong Planning Department, 2005). As shown in Figure 2, the experiment was carried out at three locations, with two zones (i.e., Zone a and Zone b) per location and evenly distributed test points within each zone to measure the overall wind VR. The overall wind VR quantitatively describes the annually averaged wind permeability in Technical Circular No., 1/06, the Air Ventilation Assessment (AVA) at Hong Kong (Hong Kong Development Bureau, 2006), and it was defined as:

$$VR = \sum_{i=1}^{16} P_i \cdot VR_{500,i} \quad (5)$$

where $VR_{500,i}$ represents the directional wind velocity ratio between wind speeds at the pedestrian level and 500 m above the ground (reference height). Second, we calculated the corresponding values of $\lambda_{f\text{-}point}$ at test points using ArcGIS, in which the pixel values of $A_{\Delta z,x,y}$ and $l_{x,y}$ were calculated using the building geometry data from Hong Kong Planning Department, and annual wind frequency data (P_i) was obtained from MM5/CALMET system (Yim et al., 2007). The $\lambda_{f\text{-}point}$ values were then entered into a linear regression analysis to predict the corresponding annually averaged wind VR.

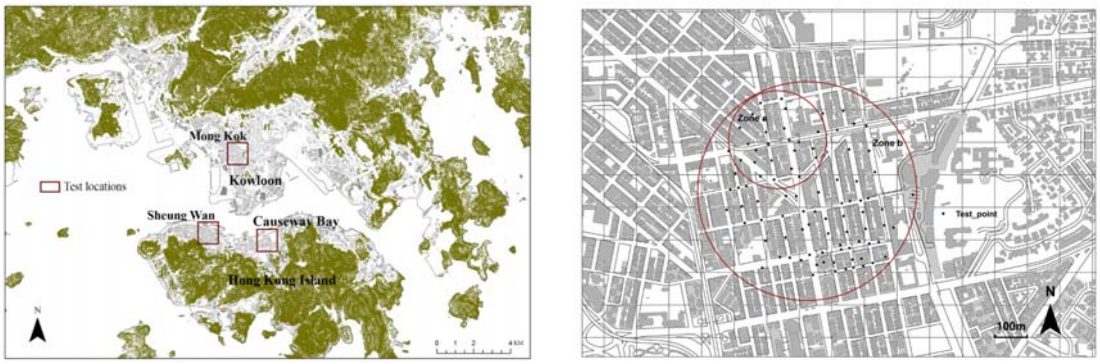

Figure 2 Three test locations. Every test location includes two zones (Zone a and Zone b) in which the test points were evenly distributed to collect the wind data.

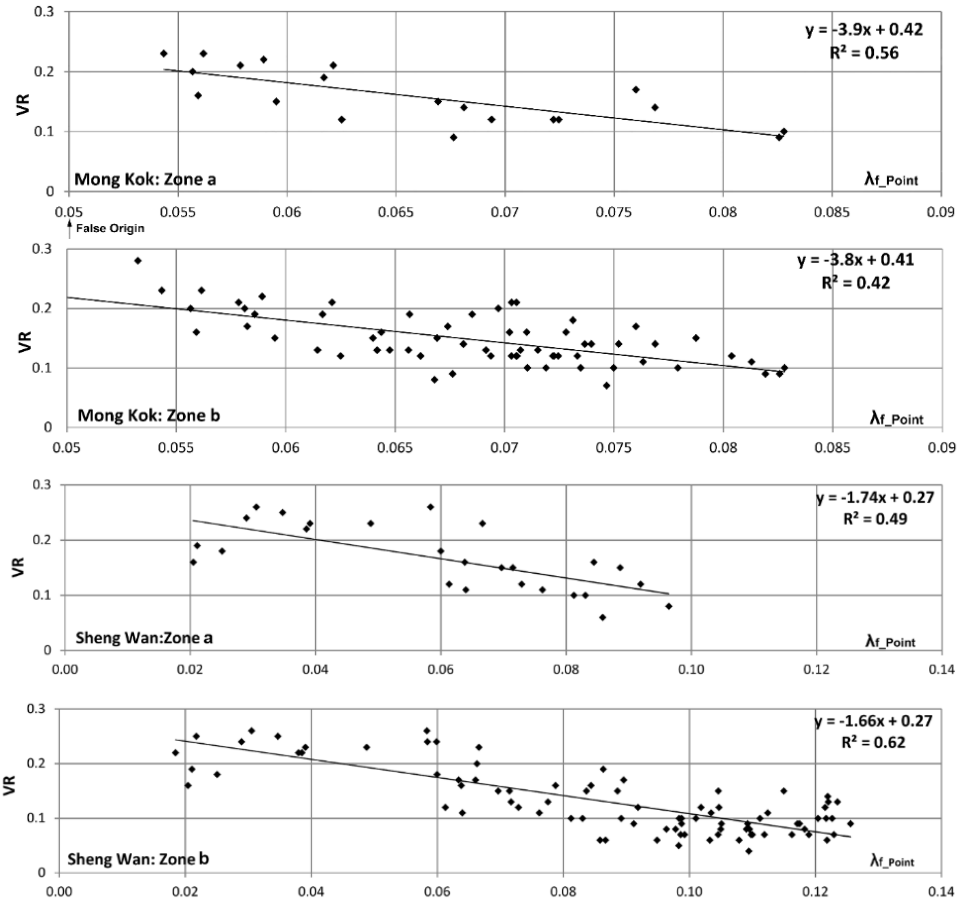

Figure 3 Linear regression analysis at Mong Kok and Sheung Wan.

Results of the regression analyses are partly shown in Figures 3 and summarized in Table 1. In general, the point-specific λ_{f_point} is negatively associated with wind VR. In other words, the closer surrounding roughness elements to the test point, the more the air flow would be impeded, and the slower the pedestrian-level wind speed at a particular point. The statistical analysis indicates an acceptable modelling-mapping method from the planning and design perspective. The urban planners and architects can use λ_{f_point} to reasonably predict the VR. The values of R^2 ranged from 0.40 to 0.62. The 95% confidence intervals (CI) of the slopes of the regression model for irregular and regular street grid are -1.66±0.14 and -3.83±0.56 respectively. The standard error (SE) of predicted VR at test zones ranged from 0.03 to 0.05. The values of CI and SE are one order of magnitude smaller than the corresponding predicted values. Assuming that the annually averaged wind speed at the reference height (500 m above the ground) at test locations is 6.67 m/s, we also calculated that the SE of predicted pedestrian-level wind speed varies from 0.20 to 0.33 m/s.

Figure 3 and Table 1 show that the slopes between street grids (regular versus irregular) differ. The slope for Mong Kok (-3.9) is significantly different from those for Sheung Wan and Causeway Bay (-1.7). The incoming air in areas with regular street grids might encounter strong resistance, and the wind speed is particularly small at streets that are perpendicular to the wind direction, given that air flow at those streets is only driven by the limited horizontal momentum transferred from the street that is aligned with the wind direction. In contrast, incoming air can easily flow around a building block in areas with irregular street grids, driven by the horizontal momentum. Thus, the same frontal area can impede more air flow in regular street grid than in irregular street grid, which explains the different coefficients and intercepts in urban areas with different street grids in Table 1. The regression analysis results also show that the slopes for different test zones within the same street grid are similar. Therefore, it is possible to develop a general regression equation to predict VR by using $\lambda_{\text{f-point}}$ for each type of street grids as shown below:

i) for districts with regular street grids (main streets perpendicular with each other)

$$VR = -3.9\lambda_{\text{f\_point}} + 0.4 \quad (6)$$

ii) for districts with irregular street grids

$$VR = -1.7\lambda_{\text{f\_point}} + 0.3 \quad (7)$$

It should be mentioned that the range of $\lambda_{\text{f-point}}$ values also depends on the street grid in the neighborhood. In the regular street grid (e.g., Mong Kok), the $\lambda_{\text{f-point}}$ range tends to be small (~0.03), especially with the similar block size and street width. In contrast, the $\lambda_{\text{f-point}}$ range in the irregular street grid (e.g., Sheung Wan and Causeway Bay) tends to be much larger (~0.08). This has significant implications in the planning and design

practice. The sizes of assessment areas should be chosen based on the $\lambda_{f\text{-point}}$ range for the corresponding street grid types. Otherwise, with too small range of the $\lambda_{f\text{-point}}$ in the chosen assessment area, the modelling result would be invalid.

Table 1 Slope Coefficient, Intercept, and Standard Error in regression equations for different districts. The result of a sensitivity test of exponent c was also presented.

Districts	Zones	R^2 (exponent c=1.0)	R^2 (exponent c=2.0)	Slope Coefficient	Intercept	SE of predicted VR	SE of predicted U_p (m/s)
Mong Kok (Grid plan)	Zone a	0.52	0.56	-3.9	0.4	0.03	0.20
	Zone b	0.14	0.42	-3.8	0.4	0.04	0.27
Sheung Wan (Irregular street grid)	Zone a	0.35	0.49	-1.7	0.3	0.05	0.33
	Zone b	0.57	0.62	-1.7	0.3	0.04	0.27
Causeway Bay (Irregular street grid)	Zone a	0.47	0.49	-1.9	0.3	0.03	0.20
	Zone b	0.40	0.40	-1.6	0.3	0.04	0.27

Note: In the calculation of SE of predicted pedestrian level wind speed (U_p), the annually averaged wind speed at the reference height (500 m above the ground) at study areas is equal to 6.67 m/s, which is from wind tunnel experiment.

4. Mapping the wind environment

Based on the above statistical analysis, we first used a self-developed program, which is embedded as a Visual Basic for Applications (VBA) script in the ArcGIS System, to calculate $\lambda_{f\text{-point}}$ using equations 1 - 4 on a pixel by pixel (1 m × 1 m) basis of all non-built-up locations in the target area. Taking Sheung Wan and Central, two metropolitan areas in Hong Kong, as an example, the results are shown in Figure 4.

Figure 4 Map of $\lambda_{f\text{-point}}$ for Sheung Wan and Central.

Figure 5 Pedestrian-level wind speed map, which was classified as Class 1 (Poor, <0.6 m/s), Class 2 (Low, 0.6 m/s -1.0 m/s), Class 3 (Satisfactory, 1.0–1.3 m/s), and Class 4 (Good, > 1.3 m/s).

Second, we extended the $\lambda_{f\text{-point}}$ map to the overall wind VR map by using regression equations 6 or 7, and calculated the pedestrian-level wind speed by multiplying VR by U_{500} (annually averaged wind speed) at the reference height, e.g. 6.67m/s at Sheung Wan and Central. Based on the physiological equivalent temperature (PET) (Cheng et al., 2011), the neighborhood wind speed field can be classified as Class 1 (Poor, <0.6 m/s), Class 2 (Low, 0.6–1.0 m/s), Class 3 (Satisfactory, 1.0 m/s – 1.3 m/s) and Class 4 (Good, >1.3 m/s). The pedestrian-level wind speed map with the classification was shown in Figure 5.

5. Implementation

The new modelling and mapping method, with its low computational cost, accuracy and high resolution modelling results, is considered as a practical tool for the urban planning in the neighborhood scale. After correlating the $\lambda_{f\text{-point}}$ with local wind data once (e.g. the wind data from the wind tunnel, CFD or field measurements), the new modelling–mapping approach enables urban planners and designers to model and evaluate the wind environment in the project by themselves, without using individual wind tunnel or CFD simulation. In this section, we illustrate the application of the new modelling-mapping approach in the air ventilation assessment (AVA) of Hong Kong. This new modelling-mapping approach can be applied in both the expert evaluation and initial study in AVA to provide a general pattern of pedestrian-level wind environment without CFD simulation or wind tunnel experiment. Modelling results can be reported as the wind velocity ratio VR or even directly the pedestrian-level wind speed, if the local wind speed at the reference height is available. Compared to the few hours or days of processing time needed for our proposed modelling method, it would take the CFD simulation or wind tunnel experiment several months to obtain a similar time averaged result (e.g., the annually-averaged results in Figure 5).

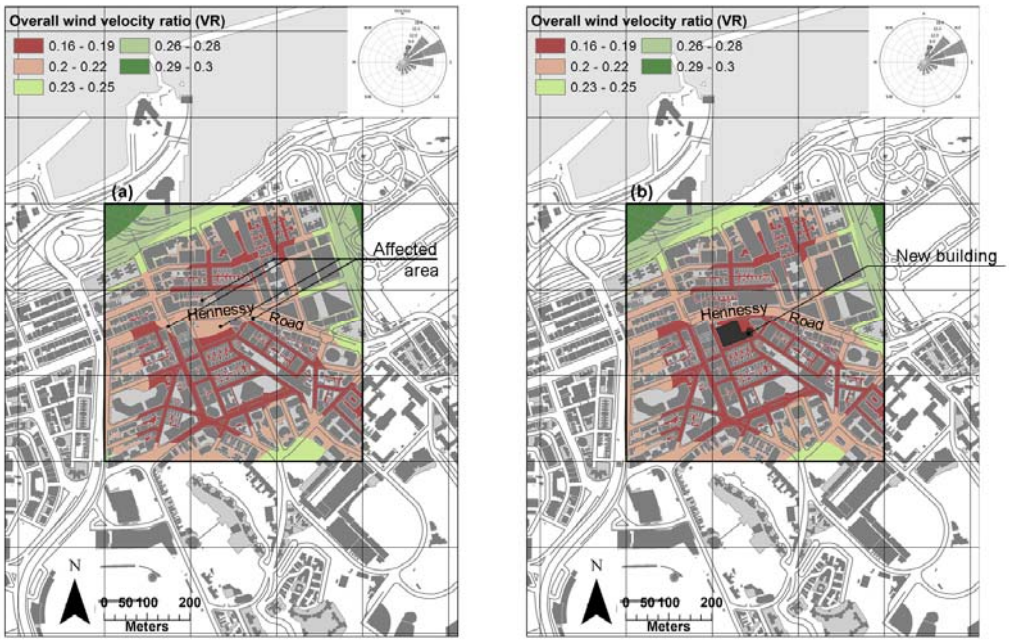

Figure 6 Evaluation of the effect of the new building on the neighborhood wind environment. (a) original scenario; (b) scenario with the new building.

First, Figure 5 quantitatively presents the wind environment at the target area. Specifically, pedestrian-level wind speed is the lowest in the deep urban areas (purple area, Class 1: <0.6 m/s) and significantly increases toward the coastal areas (dark green area, Class 4: >1.3 m/s). Based on Figure 5, urban planning and design strategies can be tailored to address specific wind environment issues at different zones. For instance, new development projects should not be allowed at the purple zone, and should be strictly controlled at the yellow zone (Class 2: Low, 0.6 m/s – 1.0 m/s) with the detailed study of AVA evaluation. Given the low air pollutant dispersion in the purple and yellow zones, planners should not arrange additional bus stops, terminus, and heavy traffic roads at these zones to avoid trapping the emitted air pollutant.

Second, urban planners and architects can apply this modelling-mapping method to evaluate the effect of a new building on the neighboring wind environment. Two scenarios were included in this case study: (a) the scenario without and (b) with new building. Figure 6 shows the new building, the surrounding street grid, and prevailing wind directions. In scenario a, the modelling results indicated poor existing wind environment surrounding the site, as depicted by the red area with VR less than 0.2, and better wind environment along Hennessy Road (i.e. the brown area with VR larger than 0.2). In scenario b, when we put a new building into the site, the red area with lower VR is enlarged in both windward and leeward direction. The affected areas are highlighted in Figure 6.

6. Conclusion and Future Work

After broadly reviewing the urban aerodynamic properties and the corresponding planning principles, we developed a modelling–mapping approach to provide fine-scale pedestrian-level wind speed between buildings. High spatial resolution modelling results and low computational cost are two attractive features of this new approach. It should be noted that the modelling-mapping approach may not be generalizable to urban densities that are different from Hong Kong (metropolitan areas). Planners should consider that following aspects before applying this approach to other cities:

a) The new approach is valid only for high density urban areas (λ_f > 0.3-0.4) (MacDonald, e al., 1998) since we developed this new approach with the assumption that the vertical momentum in the urban canopy layer can be ignored because compact high buildings interfere with each other. Therefore, the local surface roughness λ_f at the urban scale must be first investigated prior to applying this approach at other cities.

b) To calculate $\lambda_{f\text{-point}}$ in other cities, one should identify the value of Δz in the calculation of λ_f' based on the local urban morphology (Yuan, et al, 2014). The $\lambda_{f\ (0–15m)}$ (Δz: 0-15m) was applied in this study due to the specific podium morphological characteristic at Hong Kong.

c) The relationship between $\lambda_{f\text{-point}}$ and VR (i.e. slope coefficients and intercepts) could be different in other cities, given that we developed the regression equations only based on the situation in Hong Kong, and the urban densities and urban morphologies are different in other cities. Nonetheless, $\lambda_{f\text{-point}}$ is generally considered as a reasonable index to describe the local wind permeability.

d) If the local wind data is available, the same workflow in this study can be applied to develop the regression equations. The analysis results from other cities could provide insight into the sensitivity of the relation between $\lambda_{f\text{-point}}$ and VR to changes of urban densities and urban morphologies, which in turn could validate the applicability of the modelling and mapping method developed in this study to more cities.

Acknowledgment

This study was supported by the SUTD-MIT Joint-Postdoctoral Programme and the Global Scholarship for Research Excellence from the Chinese University of Hong Kong. The authors wish to thank the Planning Department of Hong Kong for providing the building data, Professor Jimmy Fung of Hong Kong University of Science and Technology (HKUST) for providing MM5 data, and Dr. Peter Hitchcock of HKUST for providing wind tunnel data. Professor Leslie Norford and Professor Rex Britter acknowledge the support of the Singapore National Research Foundation through the Singapore-MIT Alliance for Research and Technology (SMART) Centre for Environmental Sensing and Modelling (CENSAM).

References

Belcher, S. E., Jerram, N., & Hunt, J. C. R. (2003). Adjustment of a turbulent boundary layer to a canopy of roughness elements. Journal of Fluid Mechanics, 488, 369-398.

Bentham, T., & Britter, R. (2003). Spatially averaged flow within obstacle arrays. Atmospheric Environment, 37(15), 2037-2043.

Cheng, V., Ng, E., Chan, C., & Givoni, B. (2011). Outdoor thermal comfort study in a subtropical climate: a longitudinal study based in Hong Kong. International Journal of Biometeorology, in press, doi:10.1007/200484-010-0396-z.

Coceal, O., & Belcher, S. E. (2004). A canopy model of mean winds through urban areas. Quarterly Journal of the Royal Meteorological Society, 130(599), 1349-1372.

Grimmond, C. S. B., & Oke, T. R. (1999). Aerodynamic properties of urban areas derived from analysis of surface form. Journal of applied meteorology, 38, 1262-1292.

Hong Kong Development Bureau. (2006). Technical Circular No. 1/06. Air Ventilation Assessment. Hong Kong: Hong Kong Development Bureau.

Hong Kong Planning Department. (2005). Feasibility study for establishment of air ventilation assessment system, Final report. The government of the Hong Kong Special Administrative Region.

MacDonald, R. W., Griffiths, R. F., & Hall, D. J. (1998). An improved method for the estimation of surface roughness of obstacle arrays. Atmospheric Environment, 32(11), 1857-1864.

Ng, E., Yuan, C., Chen, L., Ren, C., & Fung, J. C. H. (2011). Improving the wind environment in high-density cities by understanding urban morphology and surface roughness: a study in Hong Kong. Landscape and Urban Planning, 101(1), 59-74.

Tominaga, Y., Mochida, A., Yoshie, R., Kataoka, H., Nozu, T., Yoshikawa, M., & Shirasawa, T. (2008). AIJ guidelines for practical applications of CFD to pedestrian wind environment around buildings. Journal of Wind Engineering and Industrial Aerodynamics, 96, 1749–1761.

Tominaga, Y., & Stathopoulos, T. (2011). CFD modeling of pollution dispersion in a street canyon: Comparison between LES and RANS. Journal of Wind Engineering and Industrial Aerodynamics, 99(4), 340-348.

Yim, S. H. L., Fung, J. C. H., Lau, A. K. H., & Kot, S. C. (2007). Developing a high-resolution wind map for a complex terrain with a coupled MM5/CALMET system. Journal of geophysical research, 112, D05106.

Yuan, C., Ren, C., & Ng, E. (2014). GIS-based surface roughness evaluation in the urban planning system to improve the wind environment–A study in Wuhan, China. Urban Climate, 10, 585-593.